

Pulse Shaping for Time-Domain Microwave Breast Tumour Detection: Experiments with Realistic Tissue Phantoms

Adam Santorelli, Emily Porter, Milica Popović
Department of Electrical and Computer Engineering,
McGill University
Montreal, Canada
{adam.santorelli, emily.porter}@mail.mcgill.ca,
milica.popovich@mcgill.ca

Joshua Schwartz
Department of Engineering Science,
Trinity University
San Antonio, Texas, United States of America
joshua.schwartz@trinity.edu

Abstract—In this paper, we demonstrate improved tumour detection with a time-domain microwave screening system by shaping an incident pulse. We have fabricated a synthesized broadband reflector (SBR) to provide an easily fabricated, low-cost, hardware device to reshape a generic impulse. This newly formed pulse has a specifically chosen frequency profile in order to improve signal transmission within the breast. We contrast results using this new system and our previously designed system and report on improved tumour detection when testing complex and realistic breast phantoms which consist of varying percentages of adipose and glandular tissue.

Keywords—microwave imaging; time-domain measurements; pulse shaping; cancer screening

I. INTRODUCTION

Breast cancer remains the most commonly diagnosed cancer among Canadian women. The successful treatment of the disease hinges on the early detection of the tumorous tissues. Currently, the most commonly employed screening technique is X-ray mammography, which unfortunately suffers from several drawbacks, including the use of ionizing radiation [1]. Microwave imaging techniques have been proposed as a possible complementary imaging modality to X-ray mammography to provide an early-stage breast cancer screening technique which is safe, easy to operate, and cost effective [2]. There have been several experimental microwave systems reported in the literature, [3]-[5], which have confirmed the feasibility of the technique. While the majority of these systems report on frequency domain analysis, we are focused on the use of a time-domain system, first reported in [5], since the equipment is cost-effective and a breast scan would require significantly less time.

This paper focuses on augmenting the performance of the time-domain microwave screening system by reshaping a generic impulse to a specific waveform using a microstrip line, as first presented in [6]. This technique allows for improved signal transmission through the breast tissue by matching the input signal's spectral power distribution to the frequency characteristics of the antenna. Furthermore, the use of a planar microstrip line, as opposed to bulky and expensive custom

pulse generators, offers an inexpensive hardware solution which is easily integrated with the previous system design. We report the time-domain results from measurements performed with complex life-like breast phantoms and assess improvements to the imaging system based on our ability to detect the presence of tumours within these phantom tissues.

II. BACKGROUND

Exposing the breast to electromagnetic waves in the microwave frequency range causes reflection and scattering of the incident waves. Due to the varying electrical properties within the breast structure, specifically, the contrast in dielectric properties between malignant and the healthy breast tissue [2], non-uniform scattering is observed. The low-loss nature of the fatty breast tissue allows for these signals to be recovered and used for breast image reconstruction.

We have previously reported an experimental time-domain system in [5] which excites a broadband antenna with a unipolar impulse (-7.5 V, 70 ps full width at half-maximum) created from a generic impulse generator. The mismatch between the pulse spectral content (with a significant DC component) and the antenna performance causes a significant portion of the incident power to be lost.

Previous reports, [7]-[9], have demonstrated that a passive microwave device can be fabricated to create a specific target pulse by reshaping a generic impulse. With knowledge of the spectral content of the available impulse and the frequency response of the transmitting antenna it is possible to calculate the desired response for the microstrip line. The synthesis method presented in [7] provides an exact analytical solution to convert this previously calculated frequency response to a physical profile. By modifying the shape of a microwave transmission line in agreement with the calculated physical profile, a microstrip line with the desired frequency response is fabricated. We refer to this fabricated microstrip line as a synthesized broadband reflector (SBR). An image of the fabricated SBR device is shown below in Fig. 1.

This work was supported by the Natural Sciences and Engineering Research Council of Canada (NSERC), le Fonds québécois de la recherche sur la nature et les technologies (FQRNT), and Partenariat de Recherche Orientée en Microélectronique, Photonique et Télécommunications (PROMPT).



Figure 1. A photograph of the fabricated SBR structure (not to scale). The dimensions of the device are 2.9 cm x 14.3 cm.

In [6] we have demonstrated that the SBR can be easily integrated into the time-domain system first presented in [5], and the use of the reshaped input pulse created by the SBR allows for improved signal transmission and tumour detection. In this paper, we proceed to continue this investigation on more complex and life-like breast phantoms. Additionally, we contrast the performance of this augmented system with the time-domain system from [5] when using heterogeneous breast phantoms composed of varying percentages of adipose and glandular tissue.

III. METHODOLOGY

This section will outline the various components which constitute the experimental setup and is divided into two subsections: the first section provides information about the breast phantoms used in the time-domain analysis, the second section includes details about the equipment necessary for the successful integration of the SBR device with the experimental system of [5], as well as a complete description of the experiments performed.

A. Phantom Construction

The breast phantoms are constructed from commonly available chemicals as per the instructions provided in [10]. The various components of the breast phantom, which includes fat, skin, glandular, and tumorous tissues, have been created to closely mimic, from an electrical standpoint, real breast tissues. The breast phantoms are created to perfectly fill a hemi-spherical radome.

In this paper we use four specific breast phantoms. The various phantoms are created to represent imaging scenarios which are progressively more difficult and complex. The first, and simplest, breast phantom created is a perfectly homogenous fat phantom. The second phantom consists of this same fat phantom, however, we include a 2-mm skin layer on the exterior of the breast. We have created two heterogeneous breast phantoms that are composed of 50% and 70% glandular tissue, by volume. The glandular tissue is represented by a discrete number of conical gland structures (to simulate gland geometry within the human breast). A complete description of the procedure of including glandular tissues within the hemispherical breast phantom can be found in [11]. These heterogeneous breast phantoms consist of the 2-mm skin layer with the interior of the phantom filled with the appropriate percentage of adipose tissue and glandular structures to create the desired 50% and 70% heterogeneous breast phantom.

B. Experimental System

The SBR is used to transform the input pulse so that the newly formed pulse has the majority of its power residing in the 2 - 4 GHz range. We have chosen this frequency range for two reasons: i) at frequencies below 2 GHz antenna performance is compromised ($S_{11} > -5$ dB, [5]) which severely limits the amount of power that can be delivered to the breast, and ii) at frequencies above 4 GHz the propagation loss inside the breast tissue will significantly attenuate the transmitted signal.

The SBR operates in reflection mode; the signal reflected off of the device corresponds to the desired reshaped pulse. It is necessary to use a directional coupler to recoup this reflected signal and redirect it back to the transmitting antenna. This process of deforming and re-shaping the incident pulse into a purely AC signal, as well as the routing of the signal through the directional coupler, will cause the maximum amplitude of the signal to be diminished. A broadband amplifier (+35 dB typical gain, 2 - 8 GHz) is used to counter these additional losses.

The experimental setup includes a clock operating at 25 MHz, which drives the impulse generator and sets the pulse repetition rate, as well as driving the oscilloscope. The directional coupler, SBR, and the broadband amplifier, together, form the pulse-shaping section of the experimental system. A radome is used to house the breast phantoms and the antennas; furthermore, the radome serves to improve antenna performance by providing a matching interface between the antenna substrate and the breast phantom surface. The exterior surface of the radome has 16 slots to house the antennas. These slots are separated into four equally spaced quadrants of four slots. The slots can be oriented in a parallel or perpendicular fashion, causing the antennas to be co- and cross-polarized respectively. A detailed description of each of these components can be found in [5] and [6]. A system-level schematic depicting the experimental system is shown in Fig. 2.

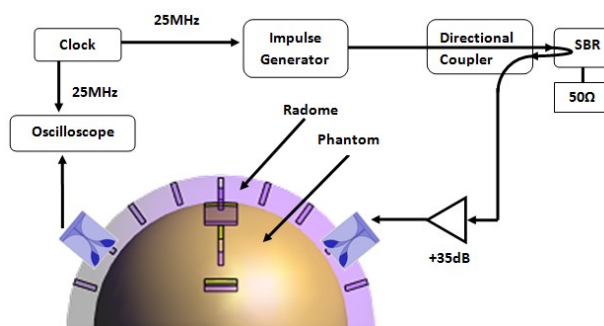


Figure 2. A high-level depiction of the experimental setup. Note that the antennas are placed within the slots of the radome.

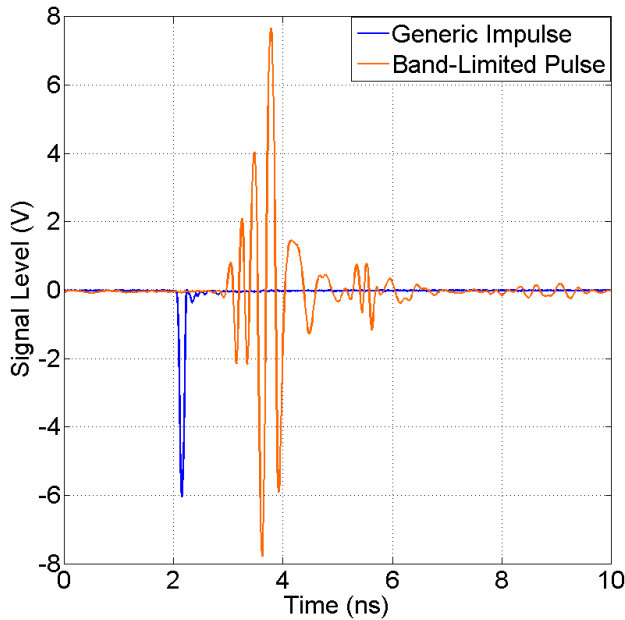


Figure 3. A comparison of the initial pulse and the reformed pulse in the time-domain.

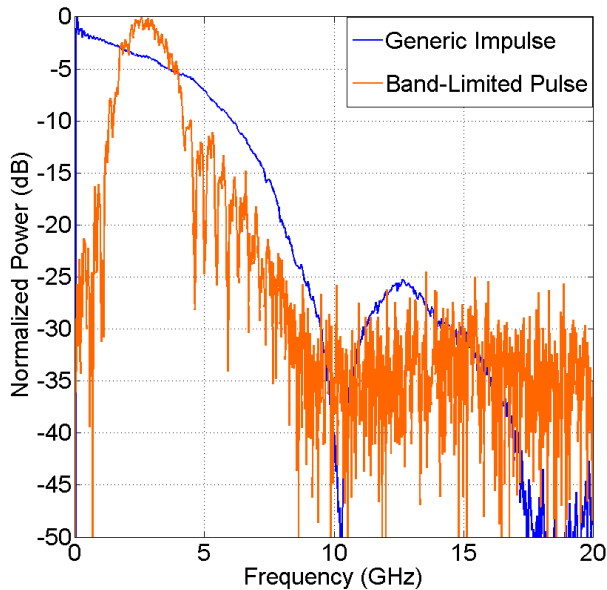


Figure 4. Frequency content of the newly formed pulse in comparison to the impulse created from the impulse generator. The majority of the signal content is now centered in the 2 - 4 GHz range, as desired.

A time-domain plot of the pulse created from the impulse generator and the newly formed, reshaped pulse is shown in Fig. 3. The frequency content of these two signals is plotted in Fig. 4. The SBR is successful in completely changing the shape of the initial impulse and focusing the majority of the content of the new signal in the 2 - 4 GHz range, strongly suppressing both the higher and lower frequencies.

We investigate the ability of the system to detect the presence of tumours in breast phantoms composed of skin, fat, and glandular tissue. Specifically, we contrast the

improvements made by implementing the SBR device within the experimental system for the four breast phantom types (fat, fat+skin, 50 % glandular, and 70% glandular) described in Section III. A. The tumour is modelled as a cylinder of 3 cm in height and of 1-cm base diameter, and is always placed 3.5 cm (half the distance from the radome wall to the phantom centre) away from the transmitting antenna.

We present the results for four specific antenna arrangements, referred to as Case 1 through Case 4. Each case refers to the specific orientation for the pair of antennas required for each measurement. From previous reports, [5], [11], it is clear that tumour detection is greatly improved when both the transmitting and receiving antennas are located on the same side of the radome (reflective scenario), hence, Cases 1 through 4 all have antennas arranged in agreement with this reflective scenario.

The pair of antennas is placed in the second and third slot from the chest wall (approximate middle of radome). For Case 1 and Case 2 the transmitting antenna and receiving antenna is located in the second and third slot, respectively, from the chest wall. For Case 3 and Case 4 the transmitting and receiving antenna are switched; the receiver is in the second slot and the transmitter is in the third slot. For Case 1 and Case 3 the antennas are oriented to be co-polarized, whereas, for Cases 2 and 4, the antennas are cross-polarized.

IV. RESULTS

Time-domain measurements are carried out for the augmented experimental system, which includes the integration of the SBR as described in Section III, as well as the experimental system described in [5]. For each of the four breast phantoms described in Section III we record two signals with each of the four cases, Cases 1 through 4 as explained in the previous section. Thus a total of 32 signals have been recorded. Of the two signals recorded for each case, the first measurement corresponds to a baseline signal. The radome is completely filled with one of the four breast phantoms, there is no tumour inserted into the phantom. This corresponds to a healthy breast. For the second measurement we insert the cylindrical tumour into the breast phantom.

We provide an example of the signal transmitted through the breast phantom, and contrast the change in the received signal when using the SBR-system when compared to the original system. Fig. 5, shown below, plots the recorded baseline signal for Case 3 when testing the 50% glandular breast phantom. This signal is recorded at the receiving antenna, after the incident microwave energy has been reflected and scattered at numerous interfaces within the heterogeneous breast structure. The use of the reshaped pulse has greatly improved the signal strength of the baseline signal, increasing the peak-to-peak voltage of the received signal from approximately 0.2 V to approximately 0.6 V.

When using the SBR-system the recorded baseline signal retains the original pulse shape after transmission through the dispersive and lossy breast tissue, in contrast to the original

system where the pulse shape has been completely deformed. This is due to the frequency response of the breast phantom itself. The tissues of the breast phantom, the glandular conical structures, the skin layer, and the adipose tissues, act as a filter with pass bands and stop bands at specific frequencies, thus transforming the spectral content of the transmitted signal and altering the signal's appearance in the time domain.

The tumour response signal is defined as the difference between the healthy baseline signal and the signal recorded when the tumour is inserted into the breast phantom. The tumour response signal is computed by subtracting the two signals from each other.

Table I compares the maximum peak tumour response signal, in mV, for both systems, across all four cases and for each of the breast phantoms under investigation. Furthermore, we include the gain, in mV, obtained by incorporating the SBR into the experimental system. The pre-shaping of the input pulse with the SBR has led to an increase in the recorded tumour response signal in each of the four breast phantoms created.

We have included, in parenthesis, the antenna arrangement that corresponds to the given signal recording. When using the SBR-system, arranging the antennas so that they are co-polarized (Case 1 and 3) improves the tumour detection ability of the system for these four breast phantoms; this can be observed based on the data presented in Table I, where each of the maximum peak tumour response signals corresponds to either Case 1 or 3. For the original system, such a claim cannot be made. In fact, as was presented in [12], for cross-polarized antennas an increase in the tumour response signal is observed.

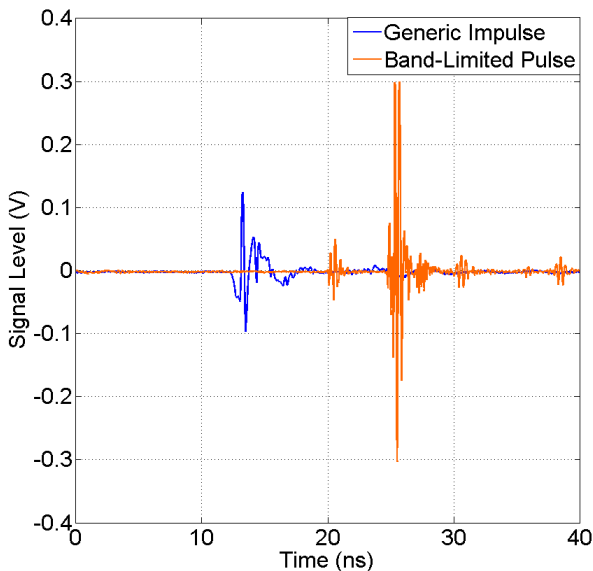


Figure 5. Time-domain measurement of the received signal for the baseline recording of Case 3. We compare the recorded signal for both the experimental system outlined in our previous work, [5], and the newly designed SBR-integrated system.

TABLE I. MAXIMUM TUMOUR RESPONSE SIGNAL COMPARISON (IN mV) ACROSS TRIALS FOR EACH PHANTOM TYPE AND EXPERIMENTAL SYSTEM

Phantom Type	Tumour Response Signal [mV]		
	Original System	SBR- system	Gain from SBR- system [mV]
Fat	19.6 (case 1)	28.2 (case 1)	+ 8.6
Fat +Skin	36.7 (case 4)	63.8 (case 1)	+ 27.1
50% Gland	12.3 (case 4)	55.6 (case 1)	+ 43.3
70% Gland	15.7 (case 4)	46.8 (case 3)	+ 31.1

Lastly, we can observe that the gain in the tumour response signal when using the SBR-system, when compared to the original system, is more pronounced in the more complex heterogeneous breast phantoms that include skin and glandular tissues. These cases correspond to the most life-like phantoms and, as such, are the most difficult to image. The original system struggles to detect the tumours in these complex models; the SBR-system greatly improves the system's tumour detection abilities in the breast phantoms which closely resemble human anatomy.

We define the relative tumour response parameter as

$$T = 20 \log \left(\frac{\max|tumour\ resp|}{\max|input\ signal|} \right), \quad (1)$$

which provides information about the strength of the tumour response signal relative to the input signal. We are interested in this metric since the two systems, with and without the integration of the SBR, have input signals of unmatched power; thus, the T parameter provides an unbiased account of the ability of each system to detect the presence of the tumours.

Table II compares the best T value, expressed in dB, for each phantom, across the four antenna arrangements, between the original system and the SBR-integrated system. Since the input is constant across trials, for each system, the antenna arrangement which led to the corresponding signal recording is identical to that in Table I.

As was evident with the tumour response signal, the integration of the SBR within the experimental system has improved the T parameter in each of the four breast phantoms under investigation. Similarly, the improvement in tumour detection is most apparent in the more complex heterogeneous breast phantoms composed of 50% and 70% gland. Furthermore, while the original system has more difficulty detecting tumours in the heterogeneous breast phantoms when compared to the homogeneous 100% fat phantom, the use of the SBR has the opposite effect; tumour detection is easier, as denoted by a larger T parameter value, for the heterogeneous breast phantoms when compared to the 100% fat phantom.

TABLE II. COMPARISON OF T PARAMETER (DB) ACROSS TRIALS FOR EACH PHANTOM TYPE AND EXPERIMENTAL SYSTEM

Phantom Type	Tumour Response Parameter, T [dB]		
	Original System	SBR- system	Gain from SBR-system [dB]
Fat	-50.16	-48.82	+ 1.3
Fat +Skin	-44.69	-41.72	+ 3.0
50% Gland	-56.02	-42.92	+ 13.1
70% Gland	-52.08	-44.42	+ 7.7

V. CONCLUSION

We have demonstrated that it is possible to easily integrate a SBR into a pre-existing experimental system in order to improve tumour detection in realistic breast phantoms. By pre-shaping and amplifying a generic impulse we are able to improve signal transmission through the complex breast structure, in turn improving the amplitude of the transmitted signal and increasing the ability of the system to detect the presence of tumours embedded within the breast phantom.

We have investigated the improvements from incorporating this pulse shaping technology on four specific breast phantoms composed of various quantities of fat, skin, and glandular tissues; specifically, for each breast phantom, four specific antenna arrangements are tested. Based on the tumour response signal, the SBR-enabled system has improved tumour detection in each of the four breast phantoms. We conclude that, when using the SBR-system, arranging the antennas such that they are co-polarized improves both signal transmission and tumour detection. Furthermore, we have observed that the improvements in tumour detection when using the SBR-system are most significant in the more complex heterogeneous breast phantoms; the most difficult imaging scenario.

These conclusions suggest that should future experiments involve the same antennas it should focus on using the SBR-system with the co-polarized oriented antennas. Future work will focus on whether these improvements in the time-domain signals correspond to improvements in quality when creating an image of the breast phantom and identifying the presence of a tumour.

ACKNOWLEDGMENT

The authors thank Dady Coulibaly for his assistance with phantom construction. We would also like to thank Israel Arnedo, Magdalena Chudzik, and Aintzane Lujambio of the Public University of Navarre for their help in the fabrication process of the SBR.

REFERENCES

- [1] Canadian Cancer Society. (2010, August 17). What is breast cancer? [Online]. Available: <http://www.cancer.ca/>
- [2] E.C. Fear, P.M. Meaney, M.A. Stuchly, "Microwaves for breast cancer detection?" *IEEE Potentials*, pp.12-18, February/March 2003.
- [3] M. Klemm, I.J Craddock, J. A. Leendertz, A. Preece, R. Benjamin, "Radar-Based breast cancer detection using a hemispherical antenna array—experimental results," *Antennas and Propagation, IEEE Transactions on*, vol.57, no.6, pp.1692-1704, June 2009.
- [4] J.M Sill, E.C. Fear, "Tissue sensing adaptive radar for breast cancer detection - experimental investigation of simple tumor models," *Microwave Theory and Techniques, IEEE Transactions on*, vol.53, no.11, pp. 3312- 3319, Nov. 2005
- [5] E. Porter, A. Santorelli, M. Coates, M. Popović, "An experimental system for time-domain microwave breast imaging," in *Proc. 5th European Conference on Antennas and Propagation (EUCAP 2011)*, Rome, Italy, April 11-15, 2011.
- [6] A. Santorelli et al., "Experimental Demonstration of Pulse shaping for Time-Domain Microwave Breast Imaging," *Technical Report: Department of Electrical and Computer Engineering, McGill University, July 2011.*
- [7] I. Arnedo, M. A. G. Laso, F. Falcone, D. Benito, T. Lopetegi, "A series solution for the single mode synthesis problem based on the coupled mode theory," *IEEE Trans. Microw. Theory Tech.*, vol. 56, no. 2, pp. 457–466, Feb. 2008.
- [8] M. Chudzik et al., "Synthesis technique for microwave circuits based on inverse scattering: Efficient algorithm implementation and application", *International Journal of RF and Microwave Computer-Aided Engineering*, vol.21, no.2, pp. 163-174, 2011.
- [9] I. Arnedo, J.D. Schwartz, M.A.G. Laso, T. Lopetegi, D.V. Plant, J. Azaa, "Passive microwave planar circuits for arbitrary UWB pulse shaping," *Microwave and Wireless Components Letters, IEEE*, vol.18, no.7, pp.452-454, July 2008.
- [10] E. Porter, J. Fakhoury, R. Oprisor, M. Coates, M. Popović, "Improved tissue phantoms for experimental validation of microwave breast cancer detection," in *Proc. 4th European Conference on Antennas and Propagation (EuCAP), 2010*, vol., no., pp.1-5, 12-16 April 2010.
- [11] E. Porter et al., "Time-Domain Microwave Breast Cancer Detection: Experiments with Comprehensive Glandular Phantoms," in *Proc. 2011 Asia-Pacific Microwave Conference (APMC 2011)*, Melbourne, Australia, Dec. 5-8, 2011.
- [12] E. Porter, A. Santorelli, M. Coates, M. Popović, "Microwave breast imaging: time-domain experiments on tissue phantoms," in *Proc. 2011 IEEE International Symposium on Antennas and Propagation (AP-S 2011)*, Spokane, Washington, U. S. A, July 3-8, 2011.